Engineering Failure Analysis 48 (2015) 41–61

Contents lists available at ScienceDirect

Engineering Failure Analysis

journal homepage: www.elsevier.com/locate/engfailanal

Numerical analysis of structural damage in the church of the Poblet Monastery

Savvas Saloustros *, Luca Pelà, Pere Roca, Jorge Portal

Universitat Politècnica de Catalunya (UPC-BarcelonaTech), Campus Norte, Jordi Girona 1-3, 08034 Barcelona, Spain

ARTICLE INFO

Article history:
Received 25 July 2014
Received in revised form 9 October 2014
Accepted 13 October 2014
Available online 6 November 2014

Keywords:
Continuum damage mechanics
Earthquake
Graphic statics
FE deformed model
Soil settlements

ABSTRACT

Identifying the possible causes of existing damage in historical structures is a complex task. Common difficulties are the limited information regarding the history of the construction, the properties of materials and the morphology of structural members. This paper investigates the capability of advanced numerical modelling to address the aforementioned issues and to simulate the damage in complex masonry structures. The case under study is the church of the Poblet Monastery, one of the UNESCO World Heritage Sites in Spain. The developed finite element model includes the actual-deformed 3D geometry of a selected bay, aiming to consider the important deformation of the structure during the analysis. Based on the historical survey, the analysis considers different hypotheses to investigate on the possible causes of existing damage: gravitational loading, settlements, past earthquakes and reported structural alterations. The influence of the material parameters on the structural safety is assessed with parametric analysis. Additionally, the parallel use of graphic statics with numerical analysis helps to interpret realistically the structure's current equilibrium. The applied numerical strategy is effective to understand the causes of the present damage in the structure. The results of the study are useful to make a first diagnosis and are the prelude for future inspection, testing and monitoring activities.

1. Introduction

The analysis of the built cultural heritage constitutes a challenging field of study. Common uncertainties regarding the material properties, the complex interaction among structural elements and the lack of historical documentation hamper the identification of the causes of damage and the evaluation of safety. Additionally, structural intervention during the inspection and restoration phases is constrained by the tangible, spiritual and cultural values of architectural heritage. Due to these particularities, international guidelines oriented to the study of heritage buildings [1–3] propose the integration of different approaches including historical survey, inspection, monitoring and structural analysis.

Structural analysis plays an important role within the aforementioned framework. It is important to identify the origin of existing damage and deformation and their effect on the structure's equilibrium, before undertaking any intervention. The analysis of the structural behaviour and damage in historical constructions is still a challenge and the range of the applied methodologies is wide and expanding [4,5]. Historically, graphic statics [6–8] and limit analysis [8–10] have been amongst the first analysis tools to study historical masonry structures. Their firm theoretical foundations and the limited demands in

* Corresponding author.
E-mail addresses: savvas.saloustros@upc.edu (S. Saloustros), luca.pela@upc.edu (L. Pelà), pere.roca.fabregat@upc.edu (P. Roca), jportal@coac.net (J. Portal).

http://dx.doi.org/10.1016/j.engfailanal.2014.10.015
1350-6307/

the knowledge of the material properties have favoured the use of these methods, which still constitute powerful techniques to evaluate the equilibrium of masonry structures (see [11,12]). However, even if these methodologies are effective to evaluate the safety and capacity of the structure, their use for the analysis of structural damage is not straightforward. This drawback has been compensated by the use of advanced computational strategies for the study of historical structures [4,13]. Among them, the Finite Element Method (FEM), and especially macro-modelling techniques, have prevailed in the analysis of large masonry structures during the last two decades [14–20]. Among other reasons, the use of FEM macro-models is supported by the fact that they constitute a good compromise between accuracy and efficiency.

Despite the growing knowledge in structural modelling and analysis, the numerical assessment of the structural damage in large historical constructions is still a non-trivial issue. Existing cracks or deformation in ancient structures may be due to the combined effect of past actions. In particular, the construction process, natural events as well as anthropogenic actions (e.g. fires, structural alterations), may possibly affect the equilibrium condition, causing damage to the structure. For this reason, the analysis of ancient structures should include the simulation of historical events and alterations, retrieved by the historical survey. In this way, the origin and the progression of the present damage can be successively assessed by modelling different scenarios such as settlements [21], long-term deformation [22], or past structural interventions [23].

Another significant difficulty in the analysis of historical structures is the representation of their current deformed geometry. Cases such as those of the cathedrals in Mallorca [22], Vitoria [24] and León [25] have demonstrated that large deformations, arising from permanent actions and past events, can significantly influence on the structural behaviour and stability. At present, this problem can be faced in two different ways. The first approach consists in the structural modelling of the investigated structure at its idealized initial non-deformed geometry. Following this, the current deformed state can be successively attained by using advanced numerical modelling of sequential actions, such as the construction process [22], and time-dependent phenomena as the creep of materials [26]. The second alternative corresponds to the geometrical modelling of the structure at its present deformed state, with the use of advanced topographical methodologies. In this way, the current deformation of the structure is considered during the structural analysis, leading to a more realistic assessment of the state of equilibrium.

The present study aims to evaluate the capability of advanced numerical techniques to simulate structural damage in complex masonry structures. In addition, this work investigates the importance of the geometrical modelling of the present deformed state in the analysis of historical structures. Finally, graphic statics is applied in parallel with finite element analysis to show the attained benefits from the conjoint use of these two approaches.

The selected case study is an important UNESCO World Heritage Site, namely the church of the Royal Monastery of Santa Maria de Poblet, situated in the municipality of Vimbodí and Poblet, in Spain. This monument is considered as an interesting example for the purposes of the current work for various reasons. Firstly, the structure presents today significant deformation and damage, which cannot be ignored throughout the numerical analysis. Secondly, the historical research on available documents has not been conclusive on the origin of this damage. Finally, the structure is characterized by large variety of materials used during past interventions and by substantial uncertainties regarding the morphology of structural elements.

The numerical analysis follows the information provided by the historical survey [27–30]. A three-dimensional finite element (FE) model of a bay of the church has been prepared including the current deformation with the use of terrestrial laser-scanning. The adopted numerical tool has been used to analyse the structure under different scenarios, such as gravitational loading, seismic forces and past structural alterations. Prior to detailed in situ testing, finite element modelling is used as a numerical laboratory to assess the most influent materials and structural characteristics. The performed analyses will be useful for a better planning of future inspection activities and monitoring to be carried out in the church.

2. The church of the Poblet Monastery

2.1. Description of the structure

The Royal Monastery of Santa Maria de Poblet (Fig. 1) is one of the three Cistercian monasteries in Catalonia, known as the Cistercian triangle, along with Santes Creus and Santa Maria de Vallbona. It was founded in 1153 by twelve Cistercian monks from Fontfroide of France, who developed the monastery using constructive and architectural solutions previously exploited in Saint-Gaal, Fontfroide, Cîteaux and Clairvaux Abbeys. It is considered as one of the biggest and most complete existing Cistercian abbeys. In addition to the monastic use, it has also served throughout the centuries as a defensive complex, a royal palace, residence and pantheon for the kings of Aragon. In 1921 the Spanish government recognized it as a national monument and since 1991 it is a World Heritage Site by UNESCO.

The plan of the church of the Poblet Monastery shows a basilica layout with a Latin cross shape (Fig. 2). The apse, the ambulatory and its five radiating chapels compose the east end. The west front consists of the main nave, with a height of 19.50 m and width of 8.40 m, and the two bracing lateral aisles at its both sides with notably lower height. The transept forms the transition between the west and east parts and provides access to the dormitory of the monks at the northern side and the new Sacristy at the southern one. The structure is considered as a typical example of the Cistercian architecture. It is based mainly on the Romanesque style but introduces some features found in the later developed Gothic style. An illustration of this synthesis are the pointed groin vaults, which roof the northern aisle and the crossing, as well as the pointed barrel vaults in the main nave and southern and northern part of the transept. The southern aisle follows a Gothic style due to its posterior addition, as it is later described.

Fig. 1. The Royal Monastery of Santa Maria de Poblet: (a) southern–eastern view of the monastic complex, (b) external view (the Nativity façade) and (c) internal view of the church.

The main material used in the masonry of the church is limestone, excavated from the local quarries of Tárrega and used in almost all the buildings of the monastic complex. The exact morphology of the masonry walls is up to date unknown. However, a comparison with other buildings within the monastic complex suggests that they are three-leaf walls with internal rubble material. The dimension stones are made of a sedimentary carbonate rock with few detrital components and varying amounts of clay matrix [31]. Their length shows large variation between 0.20 and 1.10 m while their height lies between 0.30 and 0.45 m. The arrangement of stones in the external leaves of the walls is illustrated in Fig. 3. The original mortars used in the construction are made of lime with gypsum and calcareous aggregates. The thickness of the mortar joints is about 0.01 m. Other types of mortars can be identified in the church due to numerous repairs undertaken throughout the history of the monastery, such as strongly hydraulic lime mortar or gypsum applied around inserted metallic elements [31].

In situ investigations on the roof in 2012 [32] allowed an accurate documentation of the stratigraphy of the barrel vault's infill in the main nave. The overall depth of this filling is of 1.6–1.7 m and its thickness can be subdivided into two parts. The top part is composed of an upper layer of clay tiles, a lower layer of original stone tiles and an in-between layer of sand (Fig. 4a). The upper layer of clay tiles and sand was probably added during the end of the 19th century to make up for the curvature of the deformed barrel vault in the main nave [32], as discussed later. The lower part of the filling is composed, from the top to the bottom, by layers of poor quality filling materials such as lime mortar with fragments of stone (0.65 m) and soil material (0.90 m) lying above the barrel vault (Fig. 4b). These materials can hardly contribute with a structural role except for the possible stabilizing action of their weight. The type of infill above the vaults of the lateral aisles is still unknown. This uncertainty will be carefully assessed in the structural analysis by considering two possible alternative infill materials, i.e. with and without resisting capacity (see Sections 4.1 and 4.2).

2.2. Historical survey

Fig. 5 illustrates the construction stages of the different parts of the church. The construction started in 1170 with the east end. Following the completion of this part at the end of the 12th century, the church expanded towards the west with the transept, the main nave and the two lateral aisles, finalizing the main body of the structure in 1276. Thenceforth, the church underwent several alterations and additions. During the end of the 13th century, the western entrance of the church was completed by the addition of the Galilee. Later additions to the church are also the cimborio above the crossing (15th century) and the expansion of a chapel in the southern part of the church (17th century). The façade of the Galilee was decorated in baroque style in the 18th century (see Fig. 1b).

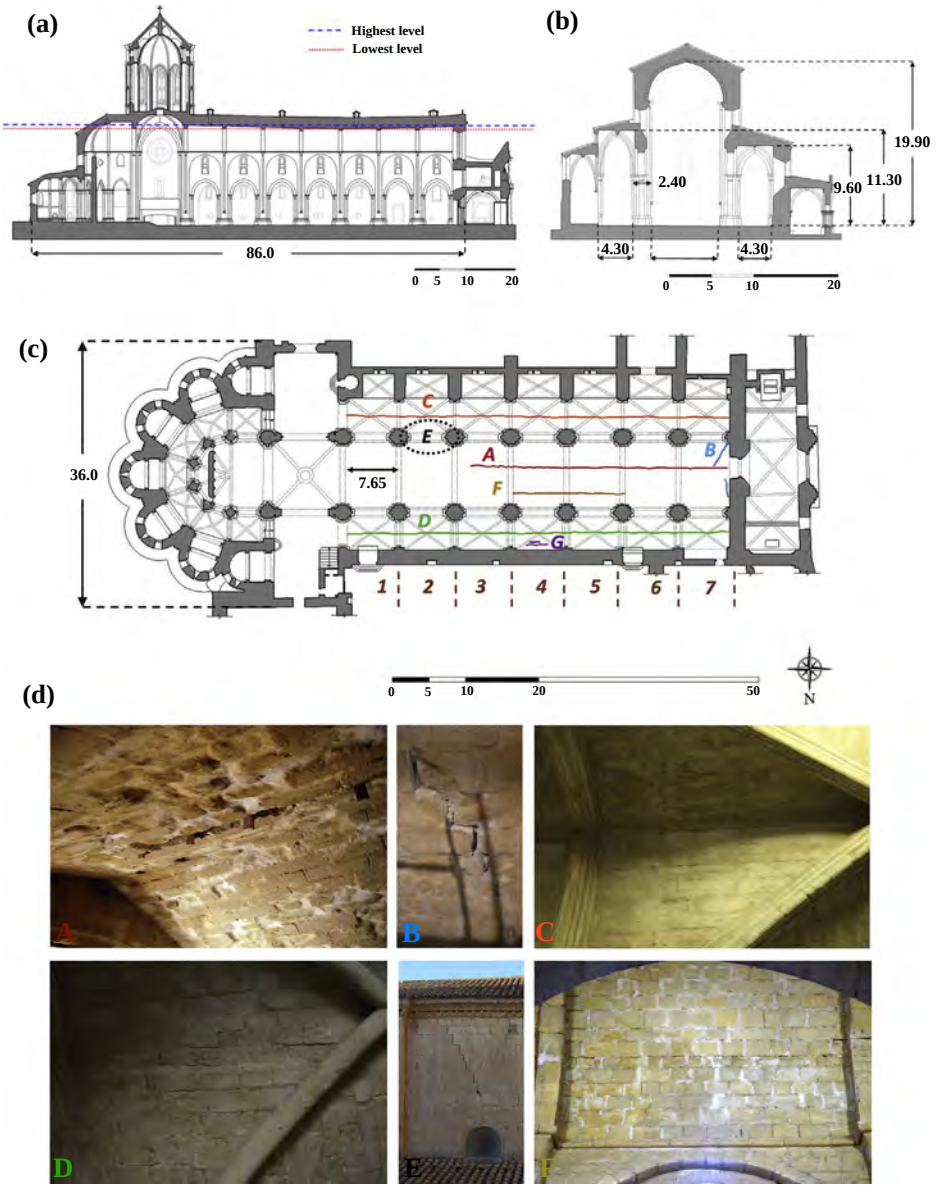

Fig. 2. (a) Longitudinal section with the deflection of the barrel vault, (b) transversal section of a typical bay, (c) plan with the cracks found within the church and enumeration of bays, and (d) pictures of cracks.

The office of Abbot Ponç de Copons marked an important era in the history of Poblet Monastery. Prominent structural additions were carried out in the whole complex. During this period and especially between 1316 and 1348, a significant alteration took place in the church of the monastery. It included the demolition of the southern aisle and its reconstruction with the addition of chapels at the southern end. Interestingly, an equivalent alteration had already occurred in the church of the Fontfroide Abbey, one of the prototypes of the church of the Poblet Monastery, with the addition of chapels communicating with the southern aisle [33]. The construction of the chapels by noble families of that time could benefit the monasteries with additional income. For this reason, these interventions might not have been related to structural problems. In any case, this structural alteration might have altered the equilibrium of the church if no provisory stabilizing system was used to counteract the thrust of the main nave after the demolition of the aisle. The difficult equilibrium of incomplete structures during the construction phases or architectural modifications posed a significant problem to master builders of the Gothic period. Different solutions were applied to overcome such difficult stages. Fitchen [34] mentions the introduction of temporary steel ties or braces in the vaults for undertaking the horizontal thrust. This scenario seems infeasible for the investigated case since no signs of such anchoring devices are visible today in the church. Another scenario has been proposed by Violet-le-Duc [35], indicating the use of large dimensioned timber struts during the construction process. These elements would

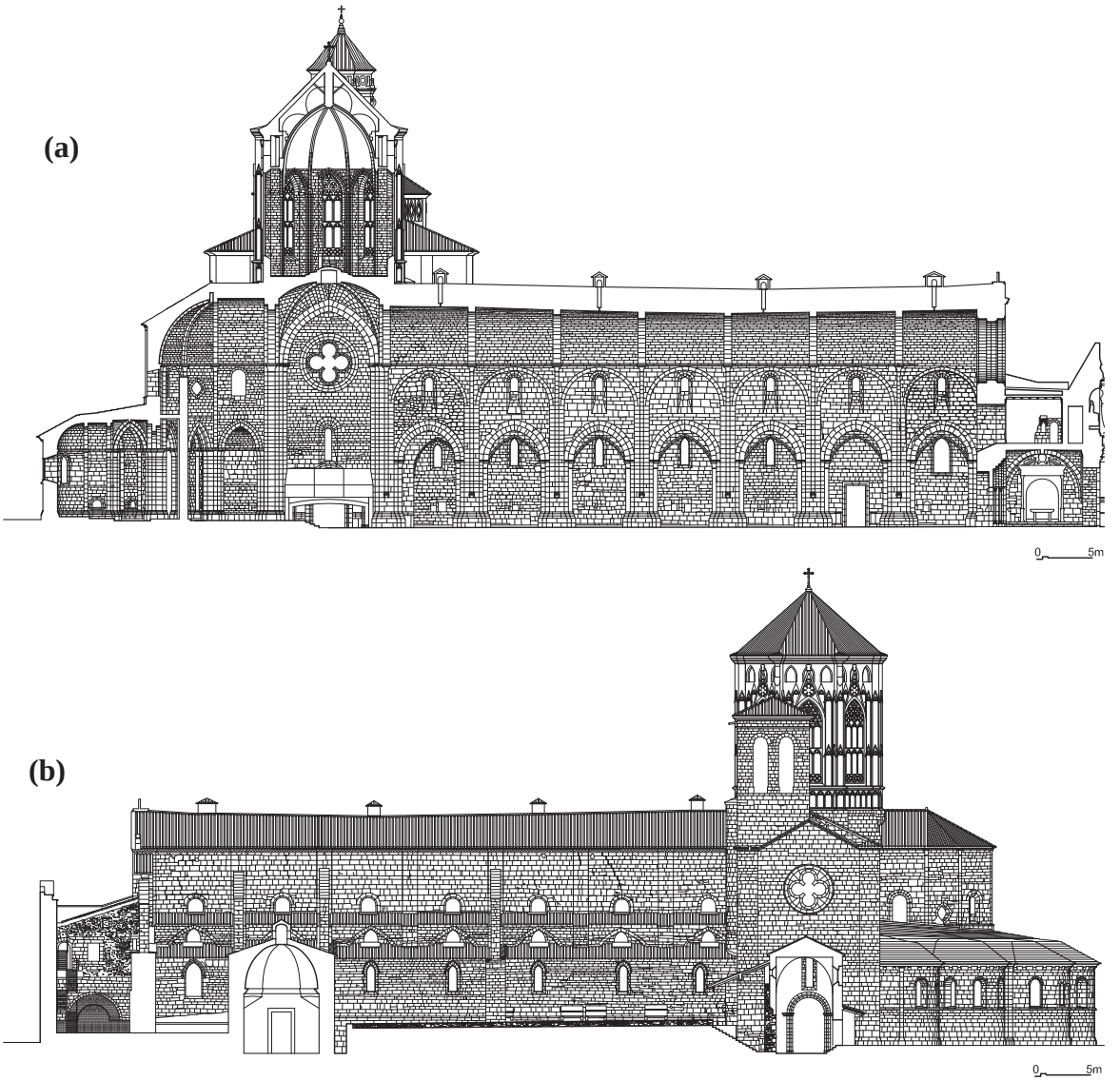

Fig. 3. Morphology of the masonry in the church of Poblet Monastery: (a) longitudinal section at the middle of the main nave and (b) external view of the southern side (Courtesy of Sánchez-López Sergio).

allow the unbalanced thrust to be safely transferred from the springing of the central barrel vault to the ground. Finally, a possible scenario could be the demolition and reconstruction of one bay at a time, without the use of any auxiliary device. In the latest setting, the tensile strength of the masonry, even though limited, could have contributed to the stability of the structure with the cost of the deformation in the main nave.

The confiscation of the ecclesiastical property, by the Spanish government in 1835, introduced an era of abandonment and plunder of the monastery. Many properties were sold in auctions, while materials were removed and used in other constructions. Within this epoch and until the rehabilitation of the church in 1940, but also during the 16th and 17th centuries, different fires contributed to further deterioration of the monastery [27,28].

The structure has undergone two major strengthening works during its life. The first took place between 1823 and 1830, and included the construction of three flying buttresses in the southern part of the church aligned with the 4th, 6th and 7th arches of the main nave as well as one buttress bracing the southern end of the western façade (Figs. 5 and 6). A possible reason for this action was to restrain the outwards rotation of the clerestory walls in the main nave. The second intervention, during the 20th century, involved the introduction of metal elements in the open joints, the cracks of the barrel vault (Fig. 7) and the piers of the southern side. Moreover, the destroyed rose window was reconstructed and damaged stones in some arches of the main nave were replaced by bricks.

Concerning the earthquake hazard, and although Spain is a country with moderate seismicity, major earthquakes have been reported in the region of Catalonia during the life of Poblet Monastery [36]. The most significant seismic events date

Fig. 4. Infill of the barrel vault: (a) upper part of clay tiles, sand and stone tiles and (b) lower part of poor quality filling materials [32].

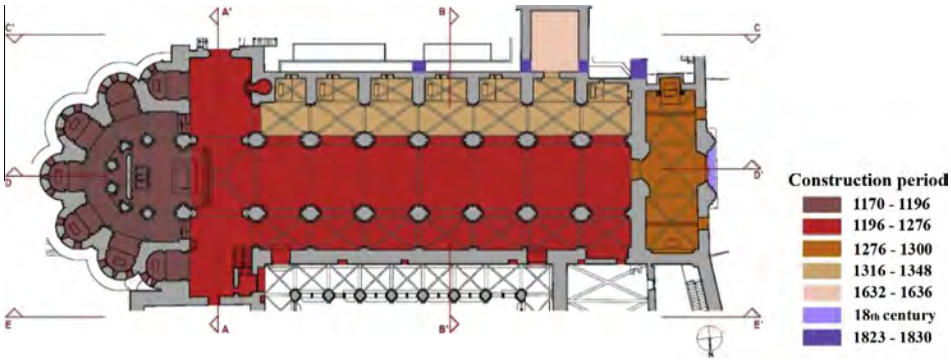

Fig. 5. Construction stages of the church of the Poblet monastery.

Fig. 6. The three flying buttresses at the southern part of the church constructed during the restoration of the 19th century.

back to the 14th century and early 15th century, with documented damage in contemporaneous churches like St. Maria del Mar in Barcelona. Additionally, an earthquake of 1792 is reported to have produced damage to the church as well as other parts of the monastery, like the dormitory located at the northern part of the transept [29].

2.3. Present damage and deformation

The combination of the previously described historical events has left evidence on the structure and especially in the main nave and in the two lateral aisles. The stone is deteriorated in many locations of the bays affected by the past fires,

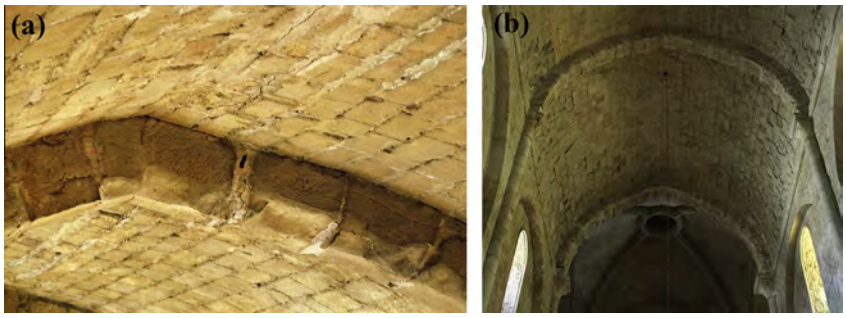

Fig. 7. (a) Metal element in an arch of the barrel vault and (b) damage by fire and metal elements in the 1st bay of the main nave.

i.e. the two adjacent to the façade and two before the transept (Fig. 7b). Unfortunately, the large amount of metal elements inserted in the mortar joints and their severe corrosion have accelerated the deterioration of the monument (Fig. 7a).

The main nave is extensively deformed. The barrel vault presents a deflection of around 0.50 m (Fig. 2a). Such deformation may be related to the outwards rotation of the clerestory walls of the main nave. In particular, the horizontal displacement at the springing of the barrel vault reaches values of 0.14 m in the southern part and 0.10 m in the northern part. The complex equilibrium state, caused by the low height of the lateral aisles, has possibly contributed to the development of this deformation (see, Fig. 2b).

Fig. 2c–d illustrate the main cracks visible in the church. The main nave exhibits a large crack close to the key of the barrel vault, which runs along the longitudinal direction and reduces its width from the façade to the transept (crack A in Fig. 2c–d). This damage is possibly related to the aforementioned deformation of the clerestory walls and the deflection of the barrel vault. Another possible cause of this crack might be the previously mentioned earthquake of 1792, as reported in [29]. Apart from this damage, the vault of the main nave presents diagonal cracks (cracks B in Fig. 2c–d) at the 7th bay (see Fig. 2c for the enumeration of the bays), which can be associated with compatibility problems in the connection between the barrel vault and the massive façade, or the effect of a past earthquake. Both lateral aisles exhibit a large crack near the key of the vaults (cracks C–D in Fig. 2c–d), crossing their whole length and showing relative vertical displacements of 5–7 cm. In the northern aisle this crack was repaired, probably during a past restoration in 1941, and has not opened again (crack D Fig. 2d). Diagonal cracking is visible over the window of the main nave in the 2nd bay from the transept (crack E in Fig. 2c–d), possibly related to the effect of past earthquakes or soil settlements. Additionally, an opening at the joints is present in the northern side of the vault at the 4th bay (crack G in Fig. 2c), which corresponds to a "Sabouret" type of cracking [9].

Some locations within the structure show crushing of the stone. This damage follows a systematic pattern at the intrados of the arches in the main nave. Moreover, in the 4th and 5th bay (with respect to the transept) this crushing is accompanied by an opening at the joints of the barrel vault (crack F in Fig. 2c–d). Finally, crushing of the stone is present in arches and architectural elements of the lateral vaults.

3. Structural analysis strategy

3.1. Geometrical modelling

The significant deformation of the church was surveyed by means of a terrestrial laser scanning. Among the principal advantages of this technique it is worth mentioning the capability to accurately capture the actual geometry of difficultly accessible parts within the structure (e.g. vaults), to avoid the contact with artistic material (e.g. frescoes, bas-relieves, sculptures) and to be easily conducted in dark spaces, like cathedrals and churches [37,38]. For this reason, it has been used in the last years for the study of ancient constructions such as palaces [17], bridges [38] and churches [39]. The result of the laser scanner survey is the geometry of the structure in the form of a cloud of points (Fig. 8).

The next step of the study was the implementation of the actual deformed geometry into the structural model. As already presented, the inspection of the church showed that the most damaged part is the western one, including the main nave and lateral aisles. Since this part of the church is composed by a sequence of equal bays, its structural behaviour, under gravitational loading, can be numerically studied by analysing a quarter of a typical bay [22,23,40]. In this work the model includes both lateral aisles and the main nave of a chosen bay due to the non-symmetrical geometry and different deformation of the lateral aisles. In particular, the selected bay is the one showing the greatest alteration, corresponding to the one under the 5th arch (4th bay). This part of the church presents the highest deflection of the barrel vault and lacks a flying buttress at its southern part. The 3D structural model has been created in a CAD environment using the results of the laser scanner survey. In this way, the current deformation of the church is directly considered in the performed analyses. The structural modelling and the post-processing have been performed with GiD [41], whereas the analysis with the FE software COMET [42]. Both software have been developed at CIMNE, Barcelona. The final adopted FE mesh is presented in Fig. 9a. It is composed by 291,101 tetrahedral elements and 61,438 nodes, with mesh refinement at the intersections of different structural elements

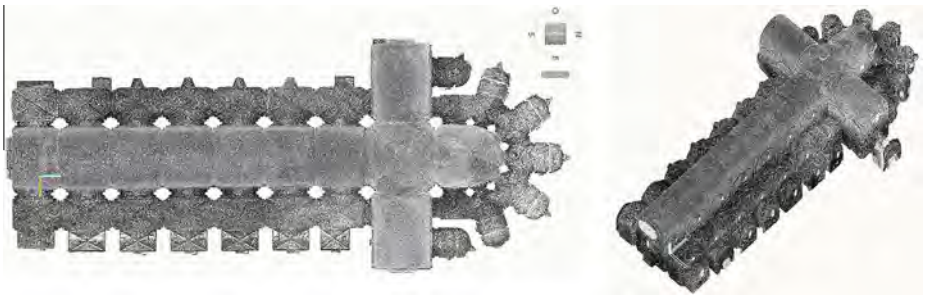

Fig. 8. Point cloud models of the church of the Poblet monastery by the terrestrial laser-scanning survey.

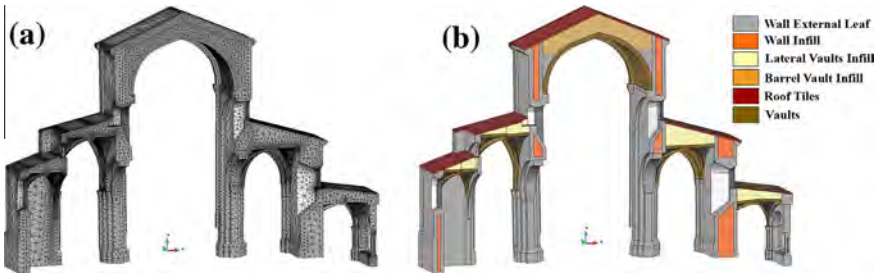

Fig. 9. Model of the investigated bay: (a) FE Mesh and (b) material distribution.

and in areas where high stress gradients are expected (e.g. vaults). It is noted that the model includes the cloister at the northern part with the aim of considering any possible interaction with the church. The confining effect of the neighbouring bays is taken into account by defining symmetry boundary conditions in the longitudinal direction.

3.2. Constitutive model

The numerical analysis considers the nonlinear response of masonry with the use of a constitutive model based on the continuum damage mechanics [43,44]. This model has been selected due to its capacity to capture the different material response under tension and compression, including softening and stiffness degradation. This is a matter of primary importance when dealing with masonry structures.

The model bases on the concept of the effective stress tensor $\bar{\boldsymbol{\sigma}}$, which in view of the strain equivalence principle [45] is related to the strain tensor $\boldsymbol{\varepsilon}$ according to the following equation:

$$\bar{\boldsymbol{\sigma}} = \boldsymbol{C} : \boldsymbol{\varepsilon} \tag{1}$$

with $\boldsymbol{C}$ denoting the (fourth order) linear-elastic tensor and (:) the tensor product contracted on two indices. The damage in the material due to tension or compression is modelled by using two scalar variables, d^+ and d^- respectively. The values of $d^{\pm}$ vary between 0 for undamaged material and 1 for completely damaged material, allowing the modelling of crushing due to compressive damage and cracking due to tensile damage. The constitutive equation can be written as

$$\boldsymbol{\sigma} = (1 - d^+)\bar{\boldsymbol{\sigma}}^+ + (1 - d^-)\bar{\boldsymbol{\sigma}}^- \tag{2}$$

In the above equation, the effective stress tensor has been split in two separate tensors, one related to tension stress states $\bar{\boldsymbol{\sigma}}^+$ and one related to compression stress states $\bar{\boldsymbol{\sigma}}^-$. Such tensors are respectively defined as

$$\bar{\boldsymbol{\sigma}}^+ = \sum_{j=1}^{3} \langle \bar{\sigma}_j \rangle \boldsymbol{p_j} \otimes \boldsymbol{p_j} \tag{3}$$

$$\bar{\boldsymbol{\sigma}}^- = \bar{\boldsymbol{\sigma}} - \bar{\boldsymbol{\sigma}}^+ \tag{4}$$

where $\bar{\sigma}_j$ stands for the j-th principal stress value from tensor $\bar{\boldsymbol{\sigma}}$ and $\boldsymbol{p_j}$ is the unit vector of the respective principal direction j. The symbol $\langle \cdot \rangle$ denotes the Macaulay brackets ($\langle x \rangle = x$ if $x \geqslant 0$, $\langle x \rangle = 0$ if $x < 0$), and $\otimes$ represents the tensor product.

In order to distinguish between loading, unloading and reloading conditions, two positive scalars, called equivalent stresses, are introduced:

$$\tau^{\pm} = \left[\bar{\boldsymbol{\sigma}}^{\pm} : \boldsymbol{\Lambda}^{\pm} : \bar{\boldsymbol{\sigma}}^{\pm}\right]^{1/2} \tag{5}$$

Table 1
Material parameters adopted in the numerical analysis for the reference model.

Structural element	γ (kg/m^3)	E (MPa)	ν (–)	f_c (MPa)	f_t (MPa)	Gf_t (J/m^2)	Gf_c (J/m^2)
External masonry leaves, vaults (Material A)	2200	2400	0.2	6.00	0.3	150	40,000
Internal masonry core (Material B)	1900	800	0.2	1.50	0.075	20	4000
Soil infill of barrel vault, roof tiles (Material C)	1800	25	0.2	0.5	0.025	20	4000

The tensors $\boldsymbol{\Lambda}^{\pm}$ define the shapes of the damage criteria in tension and compression. In this work it is assumed that $\boldsymbol{\Lambda}^{+} = \boldsymbol{p}_1 \otimes \boldsymbol{p}_1 \otimes \boldsymbol{p}_1 \otimes \boldsymbol{p}_1$, which corresponds to the Rankine criterion in tension, and for the compression $\boldsymbol{\Lambda}^{-} = \boldsymbol{C}/E$, where E denotes the Young's modulus.

Following the above, the two damage criteria can be defined as:

$$\Phi^{\pm}(r^{\pm}, \tau^{\pm}) = \tau^{\pm} - r^{\pm} \leqslant 0 \tag{6}$$

where $r^{\pm}$ are internal strain-like variables that represent the current damage thresholds and the respective expansion of the damage surface. As a consequence, their initial values are equal to the uniaxial stress under tension and compression $r_0^{\pm} = f^{\pm}$ and thereafter vary according to:

$$r^{\pm} = \max[r_0^{\pm}, \max(\tau^{\pm})] \tag{7}$$

Following the above definitions, the internal damage variables $d^{\pm}$ can be defined as:

$$d^{\pm} = 1 - \frac{r_0^{\pm}}{r^{\pm}} exp\left\{2H_d^{\pm}\left(\frac{r_0^{\pm} - r^{\pm}}{r_0^{\pm}}\right)\right\} \tag{8}$$

where $H_d^{\pm} \geq 0$ are the discrete softening parameters taking into account the compressive or tensile fracture energy of the material $G_f^{\pm}$ and the characteristic finite element length, ensuring mesh-size objective results (see [43]).

3.3. Material properties

The uncertainties regarding both the mechanical properties of the materials and the morphology of the structure (e.g. the filling over the lateral vaults) need to be carefully considered during the structural analysis of the church. For this reason, the structural assessment includes various analyses corresponding to different hypotheses on the structural morphology and the material properties.

Taking into account the features of the walls found in other buildings of the same era and importance within the monastery, the masonry of the walls of the church has been modelled as a three-leaf one. The thickness of the external leaves is 0.30 m. The infill of the barrel vault has been modelled as a unique layer and the same accounts for the upper layers of clay and stone tiles and the in-between sand. This choice follows the careful consideration of the possible effect of the different layers in the structure's response (presented in [46]). Fig. 9b reports the distribution of structural elements within the considered macro-element. The recommendations of [47,48], along with the past experience on similar structures and buildings of the monastery [49] and the nature of the masonry constituents [31] have determined the choice of the values for the mechanical properties of the modelled materials (Table 1).

The influence of the filling above the vaults of the lateral aisles has been investigated by considering two different models in the analyses. In the first model (reference model) the infill has been considered as a resisting one. In this case, the filling is defined with the properties used for the core of the masonry walls (material B in Table 1). In the second model, the infill above the vaults of the lateral aisles is modelled as a non-cohesive and not resistant one by considering the properties used for the infill above the barrel vault (material C in Table 1).

The influence of the mechanical parameters in the structural response has been evaluated with a parametric analysis, presented in Section 4.6.

4. Structural analysis results

The structural analysis includes the simulation of various scenarios which might have affected the structural integrity of the church. To analyse the response under the action of the self-weight, both the models mentioned in Section 3.3 have been used. The results are presented in Section 4.1 for the reference model and Section 4.2 for the model with poor infill above the vaults of the lateral aisles. The higher probability of a structural infill above the lateral vaults, as described in Section 4.2, has led to the use of the reference model for the analysis of the structure under soil-settlements (Section 4.3), earthquake actions (Section 4.4), and past alterations (Section 4.5).

4.1. Analysis under self-weight (reference model)

The deformation predicted by the numerical model under the self-weight is very low when compared to the deformation actually shown by the structure in its present condition. In particular, the numerical model predicts a deflection at the key of the barrel vault of 10 mm, which is far smaller than the real deformation measured at this point. This result has been expected since instantaneous numerical analyses usually predict deformations much smaller than those actually observed in ancient structures [4]. This is due to the fact that numerical models usually ignore deformations occurred throughout the history of the building, including those experienced during the construction and also deformations developed in the long-term. Recent attempts to account for those deformations have been presented in [22,26]. Consequently, this result strengthens the need of considering the true deformed geometry as the initial geometry of the structural model.

Concerning the stress state of the structure, the tensile damage derived from the analysis (Fig. 10a) is in good agreement with the damage visible in the church. In particular, the numerical analysis predicts important tensile damage, and thus cracking of the material, at the intrados of the lateral vaults and at the arches and the barrel vault of the main nave, i.e. at locations A, C and D of Fig. 2c. The numerical model predicts also a lower level of tensile damage in some other locations such as the extrados of the barrel vault as well as the infill of the northern external wall. In these cases, comparison with existing damage has not been possible due to the inaccessibility of the locations.

The overall tensile damage of the structure is related with its geometry and specifically with the low height of the lateral vaults compared to that of the main nave. In particular, the eccentric thrusts that arise within the width of the clerestory walls (see Fig. 10b) result in their outwards rotation. An immediate consequence of this deformation is the cracking at the key of the barrel vault. Along with the damage predicted at the extrados of the barrel vault, this particular cracking pattern suggests that the structure is displaying a condition of "minimum thrust state", as defined by Heyman [9]. Moving to the lateral aisles, the eccentric thrusts within both the lateral vaults (Fig. 10b) induce the present cracking at their intrados.

The compressive stresses (Fig. 11) due to the self-weight are low compared with the compressive strength assumed for the masonry. The northern springing of the vault in the southern aisle (left aisle in Fig. 11 and all the following figures) presents the highest compression, of 2.18 MPa. Other relatively high compressed areas, with decreasing magnitude, are the intrados of the arch of the northern aisle (right aisle in Fig. 11), the base of the piers, and the intrados of the arches in the main nave, with stresses between 1.2 and 2.0 MPa. According to these results, the crushing in the architectural elements (e.g. crowns of piers, arches) of the lateral aisles may be due to stress concentration in the less confined areas. In overall, though, the self-weight seems insufficient to produce the apparent crushing of the stone visible in the arches of the main nave. Consequently, different alternative scenarios have been investigated to understand the origin of this damage.

To assess the possible effect of second order phenomena another analysis has been performed considering the geometrical nonlinearity. As expected due to the low levels of deformation, both the stress and the deformation have been very similar to the geometric linear case (see [46]) and, therefore, geometrical nonlinearity has not been considered in the following analyses.

4.2. Analysis under self-weight with low mechanical properties for the infill of the lateral vaults

The uncertainty regarding the unknown type of the lateral vaults' infill has been investigated with a different numerical model. In this one, the infill is assumed to be of the same nature as the infill of the barrel vault (material C, Table 1), and thus to have a non-structural role within the church. According to the results of the numerical analysis, this scenario leads to a fragile equilibrium entailing important damage to the structure.

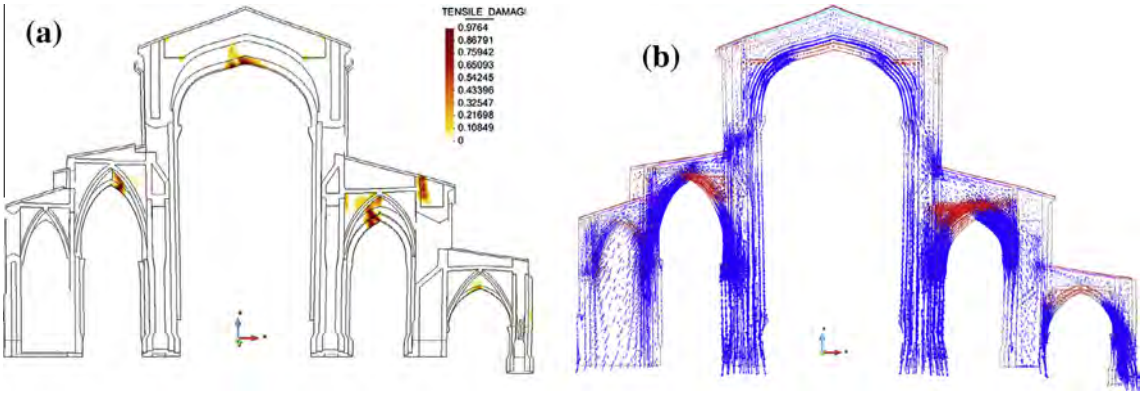

Fig. 10. Reference model under self-weight: (a) deformation (×45) and tensile damage contour and (b) vectors of principal stresses (tensile in red, compressive in blue). (For interpretation of the references to color in this figure legend, the reader is referred to the web version of this article.)

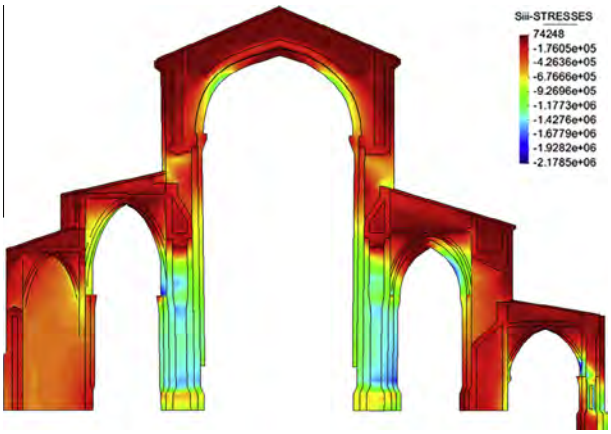

Fig. 11. Compressive stresses contour under the self-weight for the reference model.

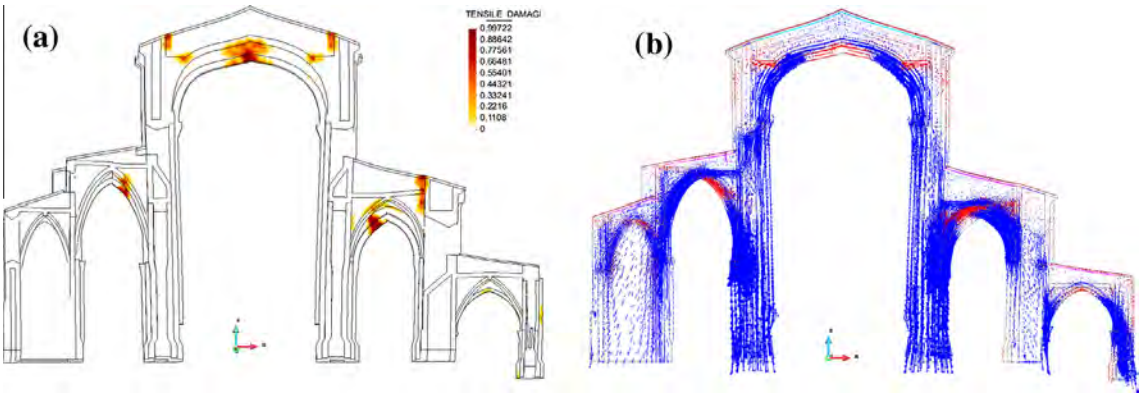

Fig. 12. Model with poor infill in the lateral vaults: (a) deformation (×45) and tensile damage contour and (b) vectors of principal stresses (tensile in red, compressive in blue). (For interpretation of the references to color in this figure legend, the reader is referred to the web version of this article.)

As Fig. 12 illustrates, the numerically predicted tensile damage is inconsistent with the one actually observed in the structure. In particular, the predicted tensile damage in the main nave is extensive and spreads over a wide area around the key of the barrel vault. The cause for this damage is the further lowering of the counteracting thrust of the lateral aisles (Fig. 12b) due to the assumed non-structural nature of their infill. Additionally, important cracking affects the northern lateral vault in a second position adjacent to the external wall. This damage pattern is not visible today in the church.

The distribution of the compressive stresses under this assumption does not present notable differences compared to the reference model. As a consequence of the new equilibrium, the values of the compressive stresses increase in areas where the thrust is close to the boundary, such as at the springing of the southern lateral vault and at the intrados of the arches in the main nave. Still the values are much below the compressive strength of the composing materials and thus no compressive damage is anticipated under the action of the self-weight.

In overall, the inconsistency between the numerically predicted damage and the damage present in the structure suggests that the infill of the lateral vaults probably consists of a more structural competent material. Nevertheless, such conclusion should be carefully assessed by an in situ inspection including the detailed characterization of the material.

4.3. Effect of differential settlements

Insufficient capacity of the bearing soil or the structure's foundation can lead to important damage in masonry structures [21,50,51]. Here, the interaction between the soil and the structure has been studied with the modelling of five possible settlement scenarios. These include settlements under the piers of the main nave and the external walls. Each analysis is performed in two steps. Firstly the self-weight is applied to the structure and secondly small vertical displacements are imposed on the base of the selected structural element.

The previous analyses under self-weight show a significant difference between the minimum principal stresses values at the base of the piers and the external walls. As should be expected, the piers of the main nave are subjected to higher compression due to their smaller cross-section and to the high loading coming from the main nave and the lateral aisles. This

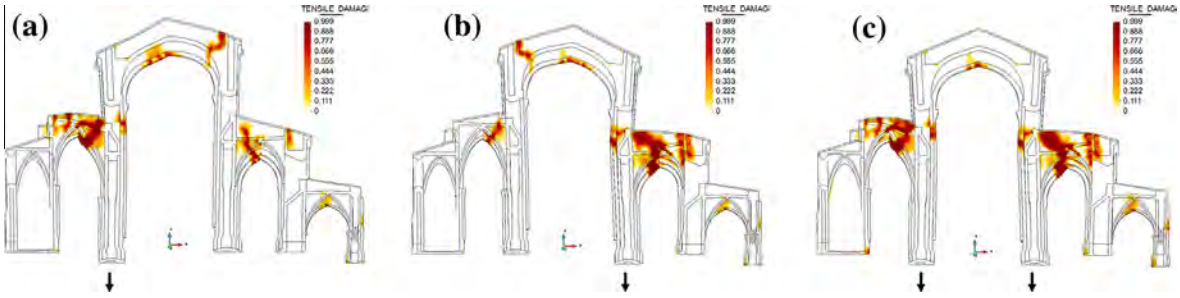

Fig. 13. Deformation (×45) and tensile damage contour for the settlement (30 mm) of the: (a) southern pier, (b) northern pier and (c) both piers of the main nave.

difference in the stress values may have resulted in a differential settlement with respect to the lateral walls. For this reason three different settlement scenarios have been numerically simulated: (a) settlement of the southern pier, (b) settlement of the northern pier, and (c) settlement of both piers of the main nave.

The results regarding the tensile damage intensity and distribution (Fig. 13, Videos 1–3) show that a settlement below the piers of the main nave would have significant effect on the lower parts of the structure. Each pier's settlement results in the further lowering of the meeting point between the thrusts of the main nave and those of the lateral nave at the side of the settlement. This change in the equilibrium affects firstly the lateral vaults. In particular, an equivalent scenario could result in the propagation of the, already open, cracks in the lateral aisles and it would produce, even for small values of settlement, cracking in the middle height of the main nave walls. The above damage is not comparable with the damage actually visible in the church. To begin with, the damage numerically predicted near the key is excessive compared with the present one. Also, the predicted damage in the walls of the main nave does not exist in the real structure. As a consequence, the numerical analyses suggest that equivalent settlement scenarios of the piers in the main nave have not occurred, at least, in meaningful values.

The same procedure used for the piers of the main naves has been used to simulate settlements below the external walls of the church. In both cases, the barrel vault is the first to be affected by the modelled settlement.

The settlement of the southern external wall results in the propagation of cracking near the key of the barrel vault and the formation of a crack at the extrados towards the intrados, at its southern side. Along with this damage, cracking starts at the springing of the southern barrel vault (Video 4, Fig. 14) that is not visible today at the structure. This discrepancy found between the damage predicted for this type of settlement and the existing damage suggests that it may not have actually occurred in a meaningful way.

As opposite to the previous scenarios, the simulation of a settlement below the northern external wall suggests that an equivalent settlement may possibly have contributed to the current damage of the main nave. In particular, the numerical model predicts that the settlement of the northern external wall could contribute to propagate the cracking near the key of the barrel vault and cause new cracking at its middle height, firstly at the northern and then at the southern side (Video 5, Fig. 15a). This simulation leads also to compressive damage at the arches in the main nave (Fig. 15b). Consequently, a similar settlement scenario may have led to the further opening of the crack A in the main nave (in Fig. 2c–d), while it could also result in the opening of joints, which is visible in some bays (crack F, Fig. 2c–d). The increase in the compressive stresses, which is observed on the arches of the main nave during the analysis, may have also contributed to the compressive damage experienced by them.

4.4. Effect of past earthquakes

Aiming to assess the possible effects of past earthquakes, different earthquake scenarios have been simulated by means of nonlinear static analysis (pushover analysis). In spite of its limitations, stemming from the modelling of the earthquake as a set of equivalent static forces, pushover analysis can provide insight on the seismic capacity and expected damage in the investigated structure. For this reason, seismic design codes have suggested its use for seismic assessment [52–54]. It is noted that the scope of the pushover analyses in the current study is to estimate the damage pattern caused by possible earthquakes and not to draw overall conclusions over the seismic capacity of the structure. For the latter case, a methodology taking into account all the structural and material uncertainties has been presented in [55].

The performed analyses include two steps involving respectively the application of the self-weight and the gradual increase of horizontal forces. Due to the planar and vertical irregularity of the investigated macro-element, the horizontal forces have been applied in two configurations: (i) proportional to the mass distribution (denoted as "Mass" in Fig. 17) and (ii) proportional to the lateral force distribution of the mode with the highest mass participation (denoted as "Modal" in Fig. 17). This methodology is consistent with the recommendations of [52] and is common in the analysis of historical masonry structures [56–58]. Due to the non-symmetrical geometry of the lateral aisles two analyses have been performed with the equivalent seismic forces respectively oriented towards the south (denoted as "−X") and towards the north (denoted as "+X").

Fig. 14. Tensile damage contour and deformation (×45) for the settlement (30 mm) below the southern external wall.

Fig. 15. Settlement (30 mm) below the northern extern wall: (a) deformation (×45) and tensile damage contour and (b) deformation (×45) and compressive damage contour.

Prior to the pushover analysis, a modal analysis has been performed aiming to obtain the modal shapes that are necessary to define the "modal" pattern distribution of the horizontal forces. The FE code MIDAS FEA [59] has been used for this purpose. Note that the geometry definition as well as the discretization are the same for all the analyses performed in this study, independent of the software. Table 2 includes the results of the modal frequencies as well as the participating masses for the first two most influencing modes in the transverse and vertical direction. The first mode (see Fig. 16 and Video 6), with a mass participation of 56.74%, is the most representative in the transversal direction and has been used to define the "modal" load pattern in the pushover analysis.

The capacity curves for the different load configurations have been compared with the capacity demand as proposed by Eurocode 8 [52]. This comparison allows a better insight on the damage experienced by the structure under a possible past seismic event at the area. The ground seismic acceleration for the municipality of Vimbodí i Poblet following the current Spanish Seismic Code [60] is 0.04 g. The soil below the church is assumed to be equivalent to that below the adjacent dormitory [48], a cohensionless one corresponding to type D as defined by the Eurocode 8. The N2 methodology [61] has been utilized to transform the capacity curves to the idealized bilinear ones of the equivalent SDOF system and to correlate them with the elastic and inelastic response spectra (Fig. 17).

As expected, the horizontal loading according to the first mode results to the lower capacity of the structure, due to the concentration of forces to the highest part of the structure. However, as Fig. 18 reports, the damage distribution for the target displacements is similar for both load configurations. Interestingly, the numerical predicted damage agrees with the existing one. In particular, the analyses suggest that a past earthquake could propagate the cracking near the key of the barrel vault and the lateral aisles. Additionally, cracking appears in a second location at the barrel vault (depending on the loading direction), at its middle height. Compressive damage is not predicted in any case for the earthquake demand. However, the numerical model predicts a high concentration of compressive stresses, with values close to the compressive strength, at the middle height of the arches in the main nave and at the arch of the lateral aisle for the pushover analysis with load distribution proportional to the first mode (Fig. 19).

The distribution of the tensile damage at the end of the analyses indicates two possible collapse mechanisms, which can develop during an earthquake event. In the analysis with horizontal loads proportional to the mass distribution, the developed mechanism corresponds to a collapse involving both the barrel vault of the main nave and one lateral aisle (Fig. 20a,

Table 2
Results of the modal analysis for the first two most important modes in the transversal (X) and vertical (Z) direction.

Mode	Frequency (Hz)	Mass X (%)	Mass Z (%)
1	0.62	56.74	0.00
3	1.30	25.60	0.08
4	1.96	0.07	26.53
6	14.47	0.08	28.97

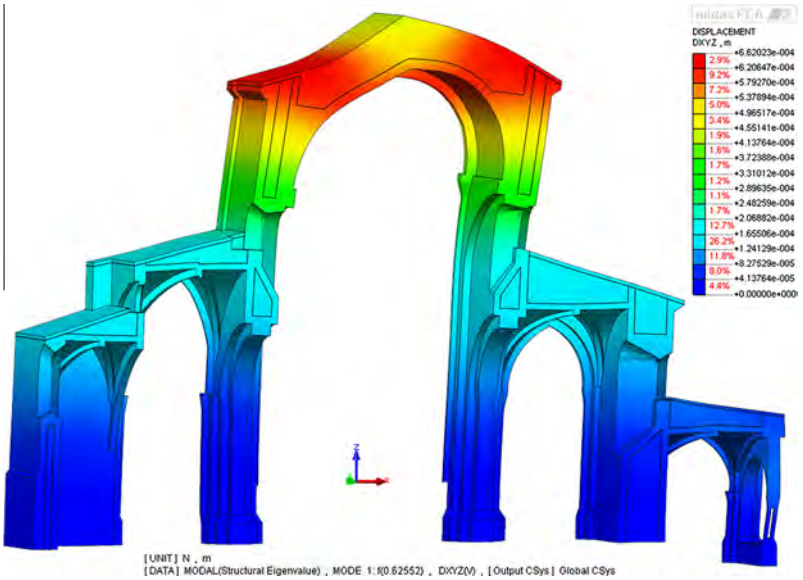

Fig. 16. First vibration modal shape of the investigated macro-element.

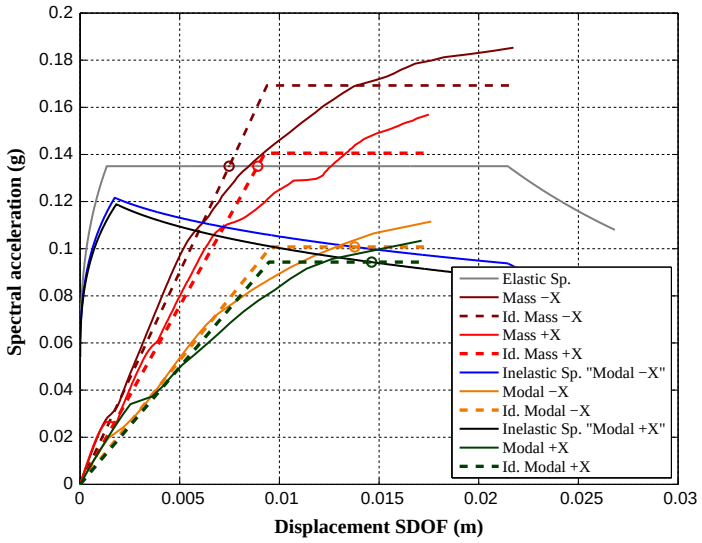

Fig. 17. Synopsis of all the capacity curves obtained by the pushover analyses (control point at the key of the barrel vault) and comparison between displacement capacity and demand, N2 method.

Video 7). On the contrary, the pushover analysis proportional to the first mode predicts the local collapse of the barrel vault of the main nave (Fig. 20b, Video 8). This scenario seems more possible due the presence of neighbouring buildings adjacent to the north of the 6th and 7th bays (Fig. 5), which may restrain the rotation of the external wall and lead to the local collapse of the barrel vault.

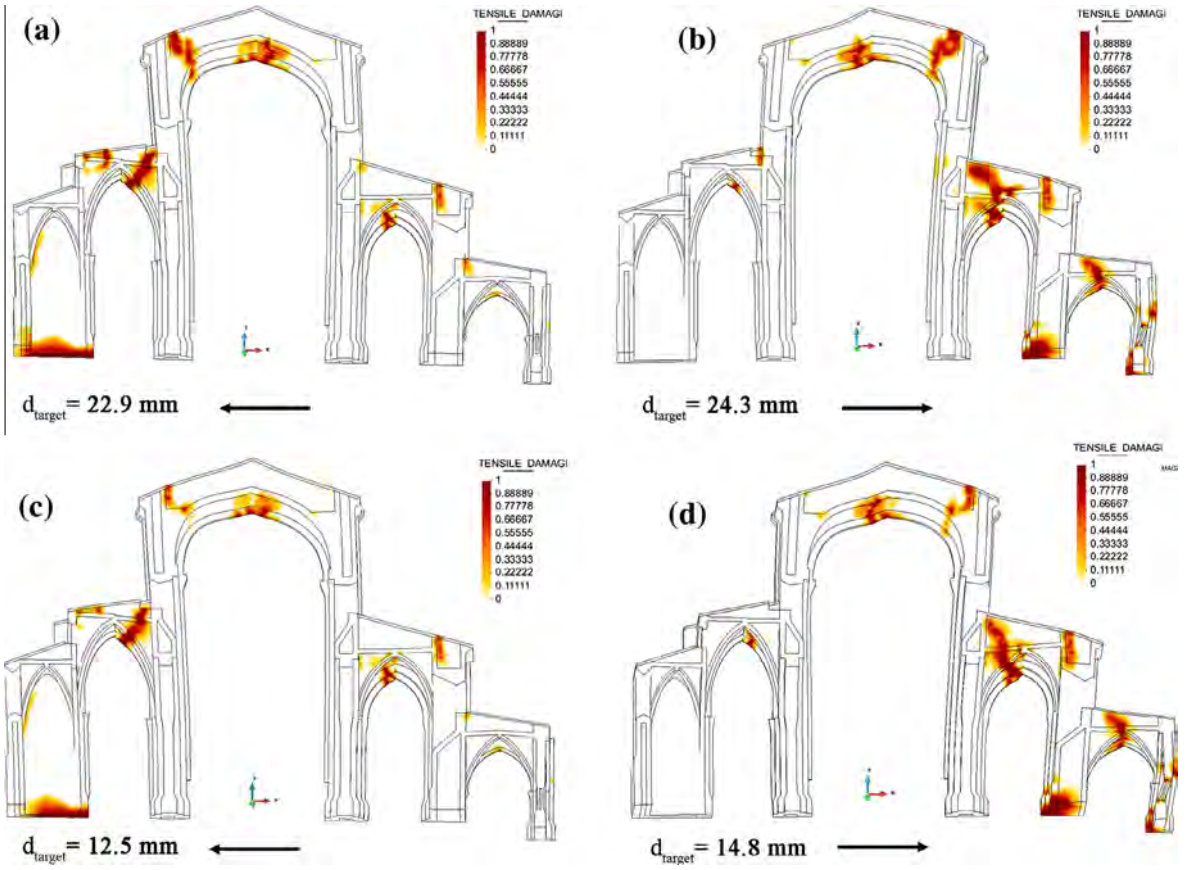

Fig. 18. Deformation (×45) and tensile damage contour for the capacity demand of the area. First mode proportional pushover analysis towards: (a) south ("Modal –X") and (b) north ("Modal +X"). Mass proportional pushover analysis towards: (c) south ("Mass –X") and (d) north ("Mass +X").

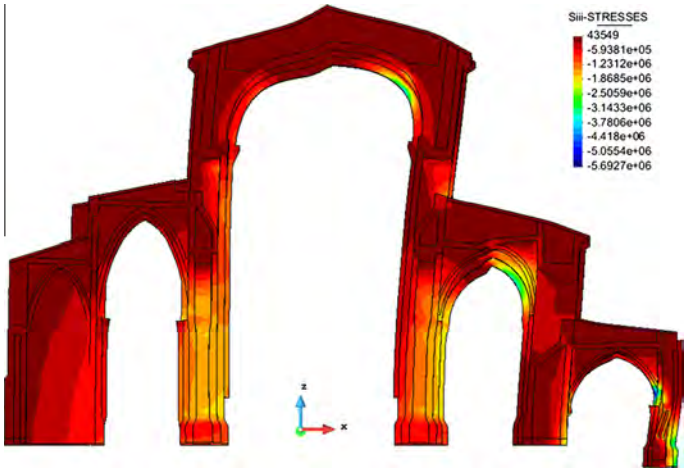

Fig. 19. Compressive stresses contour for the first mode proportional pushover analysis towards south at target displacement (d_{target} = 24.3 mm).

As a conclusion, a past seismic event can possibly have contributed to the extension of the cracking in the main and lateral aisles (cracks A, C, D, F in Fig. 2c–d). Moreover, the deteriorated condition of the stone in bays of the church affected by past fires may have made them more susceptible to crushing. This scenario is investigated in the parametric analysis presented in Section 4.6.

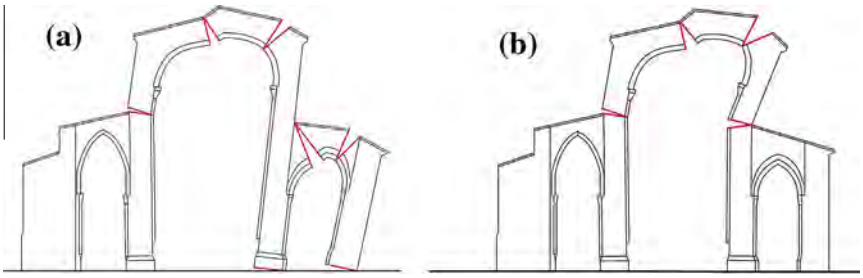

Fig. 20. Possible collapse mechanisms in a seismic event including: (a) global collapse including the main nave and one lateral aisle and (b) local collapse of the barrel vault.

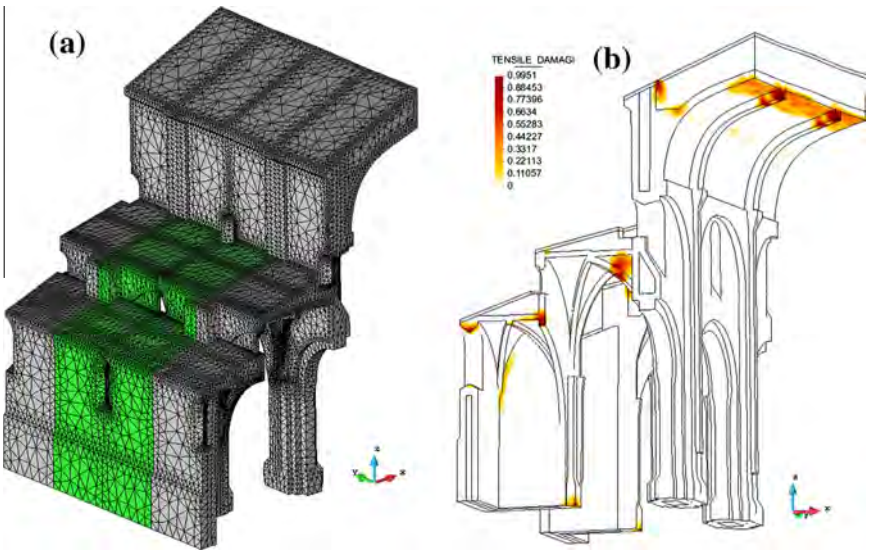

Fig. 21. Simulation of the demolition of the southern aisle: (a) FE model (in green the demolished part) and (b) deformed shape (×45) and tensile damage contour.

4.5. Effect of the demolition of the southern aisle

The demolition and reconstruction of the southern aisle was certainly a very important alteration in the history of the church. Aiming to understand the occurring effects of such an action in the remaining body of the building, a specific numerical analysis has been performed under the hypothesis of the sequential demolition of the southern aisles of each bay without the use of any auxiliary device. According to the hypothesis adopted, the aisles of each bay are reconstructed before the demolition of the subsequent bays. This analysis necessitates the use of a different model, which includes one bay of the southern half of the church and two adjacent bay quarters at each side, with a total number of 347,626 tetrahedral elements and 76,399 nodes (Fig. 21a). Appropriate boundary conditions, representing symmetry in the transverse and longitudinal direction, are defined to consider the effect of the neighbouring parts of the church. The demolition is modelled by deactivating one bay of the lateral aisle (green in Fig. 21a) after applying the self-weight in the whole model. This analysis has used a numerical strategy equivalent to that proposed in [22].

The result of the analysis provides interesting information that can be related with the present deformation and damage in the church. In particular, the analysis shows that the numerical demolition of the lateral aisle produced a sudden increase of 210% in the horizontal displacement at the springing of the barrel vault, while the deflection at the key of the barrel vault increased by 37% comparing to the state before the demolition. This deformation owns to the temporary lack of the counteracting thrust from the lateral aisle. Therefore, this result can explain the higher rotation of the southern wall in the main nave, which is actually observed when compared with the northern one, and may also have contributed to the large deflection of the barrel vault. Finally, the rotation of the clerestory wall entails the increase in the tensile damage near its key, which is clearly predicted by this analysis (Fig. 21b). Consequently, this numerical analysis suggests that the architectural modifications undertaken during the 14th century may have crucially altered the equilibrium of the structure, contributing to the deformation and damage currently visible in the barrel vault of the church.

Table 3
Range of the material parameters for the parametric analysis.

Structural element	Variable	Minimum	Maximum
External masonry leaves and vaults	E (MPa)	2000	3000
	Gf_t (J/m^2)	30	150
	f_t (MPa)	0.10	0.30
	Gf_c (J/m^2)	20,000	40,000
	f_c (MPa)	4.0	6.0
Internal masonry core and infill of masonry vaults	E (MPa)	500	1200
	Gf_t (J/m^2)	10	30
	f_t (MPa)	0.05	0.1
	Gf_c (J/m^2)	600	5000
	f_c (MPa)	0.5	1.50

4.6. Parametric analysis on material properties

The influence of the material properties adopted for the numerical analysis under gravitational and seismic loads has been investigated through a parametric analysis. The seismic analyses are performed by adopting the load distribution proportional to the first modal shape with the loads oriented towards the north. This distribution is the one that has produced the highest degree of seismic damage in the structure. The variation of the investigated material properties is illustrated in Table 3. Note that in the analyses presented hereinafter, the non-investigated parameters take the values defined for the reference model.

The results show that the variation of the parameters for the action of the self-weight affects only the intensity of the damage and not its distribution within the structure. The influence of the Young's modulus for both the investigated materials is low, affecting only the damage concentration near the key of the barrel vault. The decrease of the tensile strength and tensile fracture energy of the external leaves of the masonry and the vaults results in higher levels of tensile damage within the structure. The combination of these lower values, however, does not provide realistic conditions since it produces an overestimation of the damage actually existing in the building. Similarly, the lower values of the tensile characteristics of the infill materials result in higher damage in the infill of the lateral vaults. Finally, compressive damage affects the connections between the lateral vaults' infill and the main nave for the lower values of the compressive strength and compressive fracture energy of the infill materials. Notably, the stability of the church was not questioned for any of the investigated values.

As Fig. 22 illustrates, the most important material parameters against a seismic action are the compressive characteristics of the infill materials and the tensile characteristics of both the infill and the external wall leaves and vaults. The lowest values of tensile strength and tensile fracture energy (f_t = 0.1 MPa and Gf_t = 30 J/m^2) of the external wall leaves and vaults result in the excessive damage of the structure even for earthquakes of low intensity. However, as it is previously commented, these values are regarded as unrealistic when comparing the predicted tensile damage under the self-weight with the real one. On contrary, the decreased performance of the structure for the lower values of the compressive and tensile properties of the infill material makes it advisable to carry out further investigation on the properties of this material.

Interestingly, a seismic event could provoke compressive damage in the arches of the main nave and the lateral vaults for values of compressive strength of the external masonry leaves and vaults below 6 MPa (Fig. 23).

5. Comparison between graphic statics and FEM

Graphic statics is an appropriate and realistic tool for the safety evaluation of masonry arched structures, requiring less time and resources comparing to the numerical analysis. In this study, graphic statics have been applied to the investigated part of the church under the action of the self-weight with the aim of comparing the results with those of an equivalent FE analysis. For this reason, a FE analysis has been performed considering assumptions coherent with the graphic statics analysis, such as null tensile strength of materials. The results of this numerical analysis (Fig. 24a), have been the basis for the graphic statics solution. The latter solution has been derived with the use of an Excel spreadsheet by adjusting the position and value of the thrust in locations such as the connections between the lateral aisles and the main nave.

As Fig. 24 shows, the results of the graphic statics are in good agreement with those of the FEM, with the derived thrust line being equivalent to the distribution of the compressive principal stresses within the structure. The low height of the lateral aisles apparently results in the eccentric thrust in the clerestory walls and their respective observed rotation. Moreover, the high position of the thrust line within the depth of the lateral vaults explains the cracking experienced by them. Notably, in both cases the structure shows a satisfactory stability under self-weight, even though a null tensile strength was assumed.

6. Conclusions

The history of a monument includes a series of events that may have progressively determined its current deformation and may have crucially altered its equilibrium. The investigation of such events can supply valuable knowledge on their

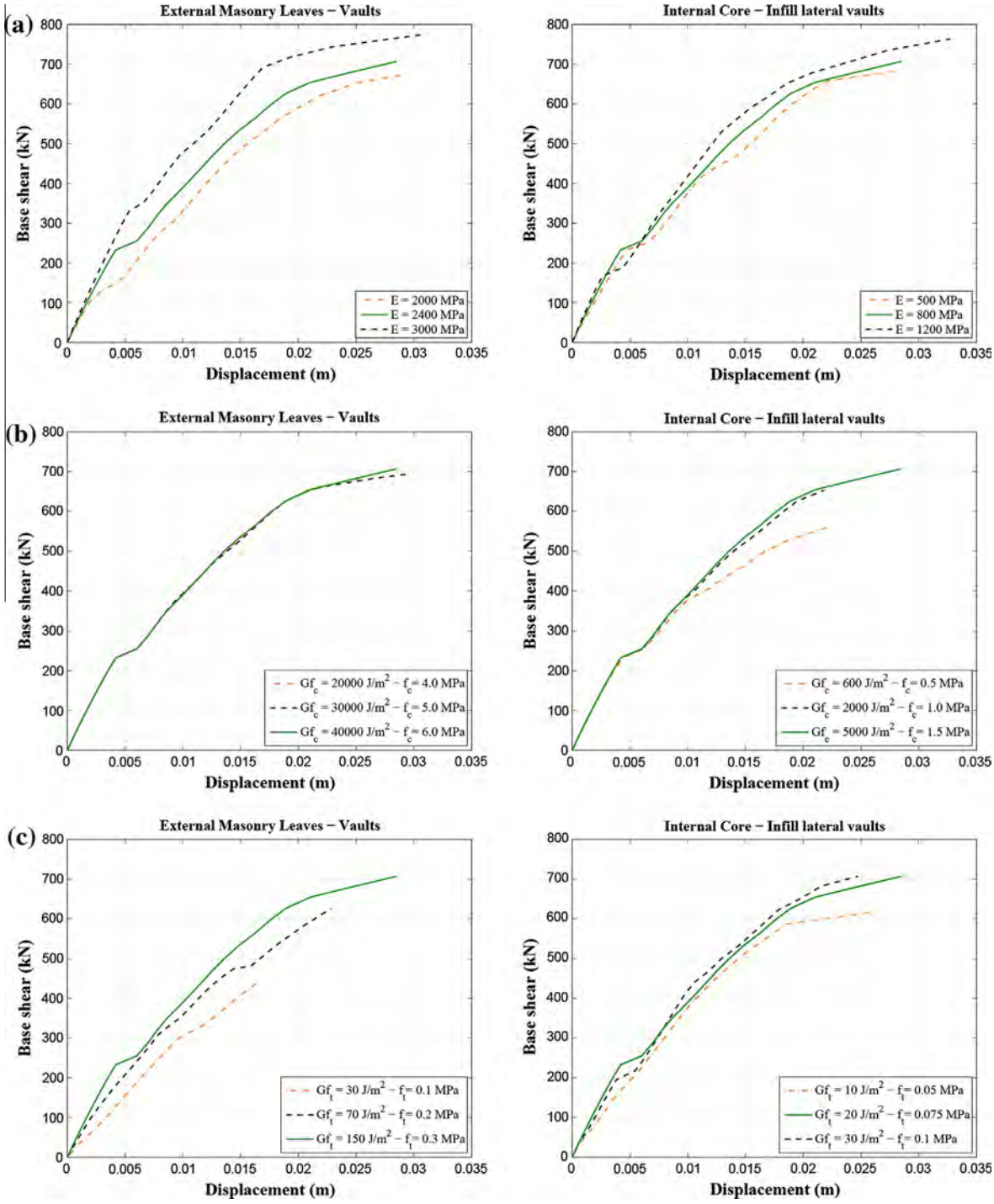

Fig. 22. Pushover curves for the variation of the: (a) Young's modulus, (b) compressive strength – compressive fracture energy, and (c) tensile strength – tensile fracture energy.

effects on the building. This is the approach that has been adopted for the assessment of the structural damage of the church of the Poblet Monastery. After the required historical and geometrical surveys, structural analysis has been carried out. The used numerical analysis tool, along with the geometrical modelling of the structure's deformed state, have provided a better understanding of the origin of the structure's damage and deformation and, therefore, its current equilibrium condition.

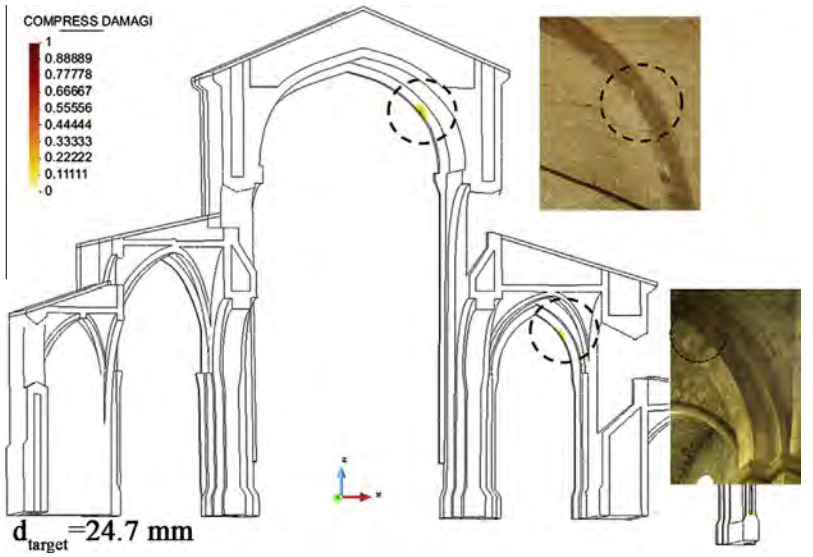

Fig. 23. Compressive damage contour at the seismic demand of the area for f_c = 4 MPa – Gf_c = 20,000 J/m^2 of the external wall leaves and vaults.

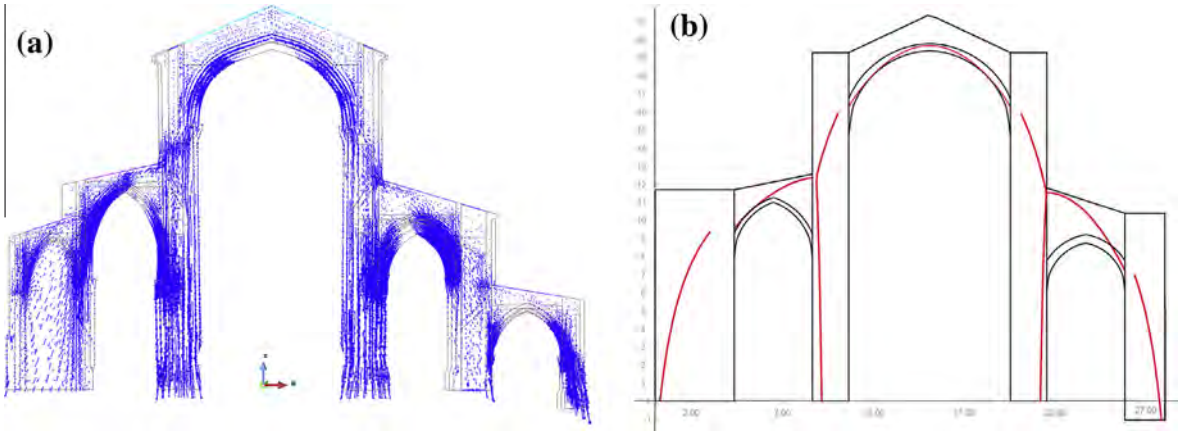

Fig. 24. Comparison FEM vs. graphic statics: (a) vectors of minimum principal stresses from FEA and (b) equivalent solution with thrust lines.

The current structural condition has been assessed by performing various analyses including the modelling of soil deformation, past alterations in the structure's geometry and earthquake actions. The analyses have shown that the most determinant parameter for the current deformation and damage on the church is the geometry of the structure and specifically the low height of the lateral vaults. In addition to this, the demolition and reconstruction of the southern aisle possibly contributed to increase significantly the damage and deformation in the main nave. Past earthquakes, although of low intensity, may have propagated the crushing in the stone in various locations within the church. The possibility of settlements at the northern part of the structure cannot be excluded, since they may have induced some damage to the vault and arches of the central nave. The analyses carried out and, particularly, the parametric analysis, point out the need to improve the knowledge on specific structural and material characteristics. Therefore, future work needs to concentrate on the identification of the structural and material characteristics of the infill above the lateral vaults, as well as that of the masonry walls. Moreover, monitoring of cracks and displacements is an important action for assessing their possible stabilization and progress. In this way, the uncertainties would sufficiently diminish and would permit future analyses with an updated numerical model.

Acknowledgments

The authors wish to thank the Comunitat Cistercenca del Monestir de Santa Maria de Poblet.

This research has received the financial support from the Ministerio de Economia y Competitividad of the Spanish Government and the ERDF (European Regional Development Fund) through the research Project MICROPAR (Identification of mechanical and strength parameters of structural masonry by experimental methods and numerical micro-modelling, Ref No. BIA2012-32234).

Appendix A. Supplementary material

Supplementary data associated with this article can be found, in the online version, at http://dx.doi.org/10.1016/j.engfailanal.2014.10.015.

References

[1] ISCARSAH Committee. ICOMOS: recommendations for the analysis, conservation and structural restoration of architectural heritage, 2003.
[2] ISO/TC98. ISO/FDIS 13822: bases for design of structures – assessment of existing structures. Genève; 2010.
[3] NIKER: New integrated knowledge based approaches to the protection of cultural heritage from earthquake-induced risk. Deliverable 10.5 Integrated methodology for effective protection and earthquake improvement of cultural heritage, December 2012 www.niker.eu.
[4] Roca P, Cervera M, Gariup G, Pela L. Structural analysis of masonry historical constructions. Classical and advanced approaches. Arch Comput Methods Eng 2010;17:299–325.
[5] Theodossopoulos D, Sinha B. A review of analytical methods in the current design processes and assessment of performance of masonry structures. Constr Build Mater 2013;41:990–1001.
[6] Huerta S. Structural design of arches, vaults and domes in Spain c.1500–c.1800. Ph. D. Dissertation, Madrid: Universidad Politécnica de Madrid; 1990 [in Spanish].
[7] Mark R, editor. Architectural technology up to the scientific revolution. The MIT Press Ltd.; 1993.
[8] Huerta S. The analysis of masonry architecture: a historical approach. Archit Sci Rev 2008;51(4):297–328.
[9] Heyman J. The stone skeleton. Int J Solids Struct 1966;2:249–56.
[10] Como M. Statics of historic masonry constructions, vol. 1. Springer Series in Solid and Structural Mechanics; 2013.
[11] Alexakis H, Makris N. Limit equilibrium analysis and the minimum thickness of circular masonry arches to withstand lateral inertial loading. Arch Appl Mech 2014;84:757–72.
[12] Alexakis H, Makris N. Structural stability and bearing capacity analysis of the tunnel-entrance to the stadium of ancient Nemea. Int J Archit Herit 2013;7:673–92.
[13] Lourenço PB. Computations on historic masonry structures. Prog Struct Mat Eng 2002;4(3):301–19.
[14] Pelà L, Aprile A, Benedetti A. Comparison of seismic assessment procedures for masonry arch bridges. Constr Build Mater 2013;38:381–94.
[15] Camata G, Cifelli L, Spacone E, Conte J, Loi M, Torrese P. Seismic safety assessment of the tower of the S. Maria Maggiore Cathedral in Guardiagrele, Italy. In: Topping BHV, Papad-rakakis M, editors. Proceedings of the ninth international conference on computational structures technology, Stirlingshire (UK): Civil-Comp Press; 2008. (Paper 58, http://dx.doi.org/10.4203/ccp.88.58).
[16] Theodossopoulos D. Structural design of high gothic vaulting systems in England. Int J Archit Heritage 2008;2(1):1–24.
[17] Mallardo V, Malvezzi R, Milani E, Milani G. Seismic vulnerability of historical masonry buildings: a case study in Ferrara. Eng Struct 2008;30:2223–41.
[18] Lourenço PB, Krakowiak F, Fernandes FM, Ramos LF. Failure analysis of Monastery of Jerónimos, Lisbon: how to learn from sophisticated numerical models. Eng Fail Anal 2007;14:280–300.
[19] Mele E, De Luca A, Giordano A. Modelling and analysis of a basilica under earthquake loading. J Cult Herit 2003;4:355–67.
[20] Meli R, Sanchez-Ramirez AR. Rehabilitation of the Mexico City Cathedral. Struct Eng Int: J Int Assoc Bridge Struct Eng (IABSE) 1997;7:101–6.
[21] Taliercio A, Binda L. The Basilica of San Vitale in Ravenna: investigation on the current structural faults and their mid-term evolution. J Cult Heritage 2007;8:99–118.
[22] Roca P, Cervera M, Pelà L, Clemente R, Chiumenti M. Continuum FE models for the analysis of Mallorca Cathedral. Eng Struct 2013;46:653–70.
[23] Roca P. Studies on the structure of Gothic Cathedrals. In: Lourenço PB, Roca P, editor. Proceedings of SAHC, vol. III., Minho; November 7–9, 2001. p. 71–90.
[24] Azkarate A, Cámara L, Lasagabaster JI, Latorre P. Plan Director para la Restauración de la Catedral de Santa Marva de Vitoria-Gasteiz. Vitoria; 2001 [in Spanish].
[25] Martínez JL, Martín-Caro JA, Torrico J, León J, The "Silla de la Reina" tower in the catedral of León. Structural monitoring combined with numerical analysis. In: Proceedings of the 12th international brick/block masonry conference. Madrid; 2000. p. 1197–208.
[26] Roca P, Cervera M, Pelà L, Clemente R, Chiumenti M. Viscoelasticity and damage model for creep behavior of historical masonry structures. Open Civ Eng J 2012;6:188–99.
[27] Domènech i Montaner L. Poblet, Montaner y Simon, Barcelona; 1916.
[28] Bassegoda i Nonell J. Historia de la Restauracio de Poblet: destrucció i reconstrucció de Poblet. Abadia de Poblet, Spain; 1983 [in Spanish].
[29] Toda E. Reconstrucció de Poblet: obres realitzades de 1930 a 1934 pel Patronat del Monestir. Barcelona; 1935 [in Catalan].
[30] Liaño E. Poblet y Santes Creus. Nuevas precisiones cronológicas y terminológicas. Boletín Museo e Instituto Camón Aznar, Zaragoza 2010;106:79–123 [in Spanish].
[31] Vendrell M, Giráldez P, Monestir de Poblet. Materials de les voltes de la nau de Íesglésia. Technical report: Patrimoni consultors 2.0, Barcelona; 2012 [in Catalan].
[32] ARCS Patrimoni Cultural SLL. Memòria de la intervenció arqueològica al Reial Monestir de Santa Maria de Poblet. Coberta Església Major (Vimbodí i Poblet, Conca de Barberà), 2012 [in Catalan].
[33] Portal J. Les églises des abbayes de Fontfroide et Poblet: modèle et déséquilibre. Actes du II Congrès Francophone d'Histoire de la Construction. Picard, Paris [in French].
[34] Fitchen J. The construction of Gothic Cathedrals: a study of medieval vault erection. Clarendon Press; 1961.
[35] Viollet-le-Duc E. La construcción medieval. Madrid: Instituto Juan de Herrera; 1996 [in Spanish].
[36] Fontserè E. Recopilació de Dades Sismiques de les Terres Catalanes entre 1100 i 1906, 1971 [in Spanish].
[37] Park HS, Lee HM, Adeli H, Lee I. A new approach for health monitoring of structures: terrestrial laser scanning. Comput-Aid Civ Infrastruct Eng 2007;22:19–30.
[38] Lubowiecka I, Armesto J, Arias P, Lorenzo H. Historic bridge modelling using laser scanning, ground penetrating radar and finite element methods in the context of structural dynamics. Eng Struct 2009;31:2667–76.
[39] Rendel M, Lüders C, Greer M, Vial I, Westenenk B, de la Llera JC, et al. Retrofit, using seismic isolation, of the heavily damaged Basílica del Salvador in Santiago, Chile, In: Wotherspoon L, Ma Q, editors. Proceedings of 2014 NZSEE conference, Auckland, New Zealand, March 21–23, 2014.
[40] Theodossopoulos D. Structural scheme of the Cathedral of Burgos. In: Modena C, Lourenco PB, Roca P, editors. Proceedings of the 4th international conference structure analysis of historical constructions, 10–13 November 2004, Padua. London (UK): Taylor & Francis; 2004. p. 643–52.
[41] GiD: the personal pre and post-processor. Barcelona: CIMNE; 2002. <http://www.gidhome.com/>.
[42] Cervera M, Agelet de Saracibar C, Chiumenti M. COMET – data input manual version 5.0. Technical report IT-308, Barcelona: CIMNE; 2002. <http://www.cimne.com/comet>.
[43] Cervera M. Viscoelasticity and rate-dependent continuum damage models. CIMNE, Monography N-79, Barcelona (Spain): Technical University of Catalunya; 2003.
[44] Faria R, Oliver J, Cervera M. A strain-based plastic-viscous damage model for massive concrete structures. Int J Solids Struct 1998;35:1533–58.
[45] Lemaitre J, Chaboche JL. Aspects phénoménologiques de la rupture par endommagement. Journal de Mécanique Appliquée 1978;2:317–65 [in French].
[46] Saloustros S. Structural analysis of the church of the Poblet Monastery. Master thesis, Spain: Technical University of Catalonia; 2013.

[47] Italian Ministry of Infrastructure and Transport. Circolare 2 Febbraio 2009, n. 617. Istruzioni per l'applicazione delle nuove norme tecniche per le costruzioni, 2009 [in Italian].
[48] P.I.E.T 70, Prescripciones del instituto Eduardo Torroja, Madrid, 1971 [in Spanish].
[49] Roca P. Monasterio de Santa Maria de Poblet: Análisis de efectos estructurales causados por sobrecargas de uso de biblioteca en el edificio del antiguo dormitorio de los monjes en biblioteca. Barcelona: UPC; 2005 [in Spanish].
[50] Macchi G. Diagnosis of the facade of St. Peter's Basilica in Rome. In: Roca P, editor. Proceedings of SAHC 1995, CIMNE, Barcelona; 2001. p. 309–18.
[51] Prabhu S, Atamturktur S, Brosnan D, Messier P, Dorrance R. Foundation settlement analysis of Fort Sumter National Monument: model development and predictive assessment. Eng Struct 2014;65:1–12.
[52] UNI ENV 1998-1 (Eurocode 8). Design of structures for earthquake resistance, Part 1: General rules, seismic actions and rules for buildings, 2003.
[53] DM 14 Gennaio 2008. Nuove norme tecniche per le costruzioni. Published on the G.U. 4 February No. 29; 2008. [in Italian].
[54] FEMA 440. Improvement of nonlinear static seismic analysis procedures. Washington: Federal Emergency Management Agency; 2005.
[55] Petromichelakis Y, Saloustros S, Pelà L. Seismic assessment of historical masonry construction including uncertainty. In: Cunha Á, Caetano E, Ribeiro P, Papadimitriou C, Moutinho C, Magalhães F, editors. Proceedings of EuroDyn 2014, Porto; June 30–2, 2014.
[56] Lourenço PB, Trujillo A, Mendes N, Ramos LF. Seismic performance of the St. George of the Latins Church: lessons learned from studying masonry ruins. Eng Struct 2012;40:501–18.
[57] Milani G, Casolo S, Naliato A, Tralli A. Seismic assessment of a medieval masonry tower in Northern Italy by limit, nonlinear static and full dynamic analyses. Int J Archit Heritage 2012;6(5):489–524.
[58] Betti M, Vignoli A. Numerical assessment of the static and seismic behaviour of the basilica of Santa Maria all'Impruneta (Italy). Constr Build Mater 2011;25(12):4308–24.
[59] MIDAS FEA v. 1.1. Advanced nonlinear and detailed analysis program. User manual.
[60] Comisión Permanente de Normas Sismo resistentes. Norma de construcción sismo resistente NCSE-02, Real Decreto 997/2002. Madrid: Spanish Ministry of Public Works; 2002 [in Spanish].
[61] Fajfar P. A nonlinear analysis method for performance-based seismic design. Earthq Spectra 2000;16:573–92.